Naceur *et al. Geoscience Letters* (2022) 9:39
https://doi.org/10.1186/s40562-022-00249-4

Geoscience Letters

RESEARCH LETTER

Open Access

Performance assessment of the landslide susceptibility modelling using the support vector machine, radial basis function network, and weight of evidence models in the N'fis river basin, Morocco

Hassan Ait Naceur[1], Hazem Ghassan Abdo[2,3,4*], Brahim Igmoullan[1], Mustapha Namous[5], Hussein Almohamad[6], Ahmed Abdullah Al Dughairi[6] and Motrih Al-Mutiry[7]

Abstract

Landslides in mountainous areas are one of the most important natural hazards and potentially cause severe damage and loss of human life. In order to reduce this damage, it is essential to determine the potentially vulnerable sites. The objective of this study was to produce a landslide vulnerability map using the weight of evidence method (WoE), Radial Basis Function Network (RBFN), and Support Vector Machine (SVM) for the N'fis basin located on the northern border of the Marrakech High Atlas, a mountainous area prone to landslides. Firstly, an inventory of historical landslides was carried out based on the interpretation of satellite images and field surveys. A total of 156 historical landslide events were mapped in the study area. 70% of the data from this inventory (110 events) was used for model training and the remaining 30% (46 events) for model validation. Next, fourteen thematic maps of landslide causative factors, including lithology, slope, elevation, profile curvature, slope aspect, distance to rivers, topographic moisture index (TWI), topographic position index (TPI), distance to faults, distance to roads, normalized difference vegetation index (NDVI), precipitation, land use/land cover (LULC), and soil type, were determined and created using the available spatial database. Finally, landslide susceptibility maps of the N'fis basin were produced using the three models: WoE, RBFN, and SVM. The results were validated using several statistical indices and a receiver operating characteristic curve. The AUC values for the SVM, RBFN, and WoE models were 94.37%, 93.68%, and 83.72%, respectively. Hence, we can conclude that the SVM and RBFN models have better predictive capabilities than the WoE model. The obtained susceptibility maps could be helpful to the local decision-makers for LULC planning and risk mitigation.

Keywords: Landslide susceptibility, GIS, Weight of evidence (WoE), Support vector machine (SVM), Radial basis function network (RBFN), Morocco

Introduction

Landslides are considered one of the most significant geological and geomorphological events threatening the sustainability of environmental quality, especially in mountainous areas. Landslide events are accelerated as a result of the complex integration between physical factors and human activities (Zhang et al. 2022). Landslides are determined as an occurrence or sequence of

*Correspondence: hazemabdo@tartous-univ.edu.sy

[2] Geography Department, Faculty of Arts and Humanities, Tartous University, Tartous, Syria
Full list of author information is available at the end of the article

occurrences where a rock mass and debris fall or flow down a slope (Silalahi et al. 2019). Landslides lead to life loss, the depletion of natural resources, and the destruction of infrastructure (Guzzetti 2005; Varnes 1978; Bourenane et al. 2016; Rahman et al. 2022). Compared to other physical disasters, like earthquakes, floods, and volcanoes, landslides are much more frequent and influential (Abdo HG 2022).

Recently, landslides have attracted attention since representing the most prevalent hazard worldwide related to damaging society and the economy (Nefesliogl u et al. 2008; Shahabi et al. 2014). Moreover, governments around the world are trying to find and develop safeguards to manage the landslides risk. The spatial prediction mapping of landslide susceptibility is one of the most effective methods for maintaining slope stability. Landslide susceptibility mapping is the spatial distribution of the possibilities of landslide occurrences in a specific location supported by statistical methods and local causative geo-environmental parameters (Wang et al. 2015). In this regard, landslide susceptibility evaluation and mapping are important tools in landslide risk management, assisting authorities, practitioners, and decision-makers in developing a more sustainable and appropriate land use and risk mitigation strategy, including the implementation of surveillance and warning systems (Roccati et al. 2021).

Many approaches have been globally developed to assess landslide susceptibility mapping. Recently, statistical methods based on the use of geographic information systems (GIS) and remote sensing (RS) data have become popular in the assessment of landslide susceptibility, such as fuzzy logic and the analytical hierarchical processes (FAHP) (Abdı et al. 2021); certainty factor (CF) (Soma and Kubota 2018); logistic regression (LR) (Aditian et al. 2018a); index of entropy (IoE) (Wang et al. 2016a, b); multi-criteria decision analysis (MCDA) (Nsengiyumva et al. 2018); statistical index (SI) (Zhang et al. 2016), frequency ratio (FR) (Chen et al. 2016; Abdo HG 2022), certainty factor (CF) (Kanungo et al. 2011), and the information value (IV) (Manchar et al. 2018).

Moreover, among probabilistic methods, machine learning techniques have become popular in recent years. Machine learning is an artificial intelligence discipline that effectively overcomes the constraints of data-dependent bivariate and multivariate statistical methods (Park et al. 2019). They are recommended because they do not require prior elimination of anomalies, data manipulation, or statistical assumptions. These algorithms automatically identify interactions between landslides and causal causes. Several studies have found that these strategies produce more accurate predictions than standard statistical methods (Pourghasemi and Rahmati 2018).

These data-driven techniques are based on artificial intelligence algorithms (AIA) that use a high repetition rate of modelling processes, so allow analysis and predict information by learning from training datasets (Ghasemian et al. 2022). Various machine learning models were employed to map landslide susceptibility, such as artificial neuronal networks (ANNs) (Wang et al. 2016a, b; Pham et al. 2017a, b; Aditian et al. 2018a), fuzzy logic (FL) (Shahabi et al. 2015), neuro-fuzzy (NF) (Dehnavi et al. 2015; Chen et al. 2019), random forest (RF), decision tree (DT) (Tien Bui et al. 2016), maximum entropy (ME) (Park 2015), support vector machine (SVM) (Dou et al. 2019); general linear model (GLM) (Pourghasemi and Rahmati 2018), adaboost (AB) (Micheletti et al. 2014), multivariate adaptive regression splines (MARS) (Conoscenti et al. 2015), and the group method of data handling (GMDH) model (Jaafari et al. 2022a, b).

In Morocco, N'fis basin is considered one of the areas most exposed to natural hazards, as many studies indicated (Gourfi and Daoudi 2019; Meliho et al. 2020; Karmaoui et al. 2021). In this regard, the slopes of N'fis basin are exposed to severe geomorphological hazards due to the influence of a combination of physical and human geographical factors (Igmoulan et al. 2022). Landslide is one of the most frequent types of slope material movement in the study area. The spatial conducted investigations indicate the seriousness of the spatial consequences of the landslide events, especially on the lives and infrastructure. Thus, landslide susceptibility mapping is among the most important procedures for managing this acute spatial challenge.

Based on the issue discussed above, the principal goals of the present study are to produce landslide susceptibility maps using SVM, RBFN, and WoE models and to compare their performances for the N'fis basin in Morocco. The principal difference between the current assessment and the described techniques in the aforementioned publications is that three used models have never been explored for landslide modelling in the high Atlas region. Also, the performance comparison of these models is not found in the literature, thus enhancing the research values in this study. These contributions, however, provide a significant contribution to the scientific community. In addition, these landslide susceptibility maps delineate areas vulnerable to landslide phenomena, allowing planners to select appropriate locations for future development projects.

Literature review: Morocco context

In Morocco, several studies presented an assessment of the spatial susceptibility of landslides, which constituted a critical research advance in terms of data, tools, methods, and accuracy of results. In this regard, these studies have gained importance in landslide threat mitigation in mountainous areas. Field studies, including geological and topographical assessments, formed a solid basis for assessing the landslide risk in several regions in Morocco) Rouaia and Jaaidi 2003; El Khattabi and Carlier 2004). Similarly, Elmoulat et al. (2021) reported the effectiveness of a Mass movement susceptibility mapping method in landslide modelling on a large scale in the Tétouan province. Furthermore, El Jazouli et al. (2022) determined the liquid limit values (28% and 56%) and the mean plasticity index of the units (13%–24%) as a result of the significant effect of precipitation intensities and unconsolidated soil characteristics in increasing landslide events in the high basin of Oum Er Rbia in the Middle Atlas Mountain. The integration of bivariate statistical methods and geographic information system (GIS) has been used in many landslide vulnerability studies. Boualla et al. (2019) utilized GIS matrix method (GMM) to produce a spatial sensitivity map of landslides in the Safi region, West Morocco. Also, Bousta and Ait Brahim (2018) presented a spatial assessment of landslides using the Weights of evidence method in the Tangier area that witnesses a high intensity of landslide events. Elmoulat and Ait Brahim (2018) confirmed the high quality of a WoE method in mapping a landslide susceptibility map in the Tetouan-Ras-Mazari area (Northern Morocco). Es-Smairi et al. 2022 demonstrated that the information value (IV) method has achieved the highest accuracy compared to the statistical index (SI), weighting factors (WF), and evidential belief function (EBF) models in the spatial analysis of landslide hazard in the Rif chain (northernmost Morocco). The landslide susceptibility mapping of a physically based (PB) method has been improved in Al Hoceima, Northern Morocco using the Monte Carlo (MC) method backed with sensitivity analysis (SA) (Rahali 2019).

The coupling between the Analytic Hierarchy Process (AHP) method and GIS with diverse spatial data sources produced enhanced spatial outputs related to the landslide vulnerability in the mountainous regions of Morocco, such as the peninsula of Tangier, Rif-Northern Morocco (Brahim et al. 2018), Oum Er Rbia high basin (El Jazouli et al. 2019), Oued Laou watershed (Semlali et al. 2019), parts of the Rif chain, northernmost Morocco (Es-smairi et al. 2021), and the Province of Larache (El Hamdouni et al. 2022). Furthermore, Ozer et al. (2020) presented the first application of hierarchical fuzzy inference systems (HFIs) in expert-based landslide susceptibility mapping in a data-scarce region in the central part of the Rif Mountains (Morocco). Benchelha et al. (2019a, b) compared between logistic regression (LR) and multivariate adaptive regression spline (MarSpline) methods in landslide susceptibility mapping in Oudka, Northern Morocco, and the result indicated that the MarSpline model is a better model than the LR model.

Recently, a few studies have attempted to investigate landslide susceptibility using the integration between artificial intelligence algorithms (AIA) and GIS in response to global advances in this field. Machichi et al. (2020) demonstrated that the artificial neural network (ANN) method has achieved the best performance in assessing the landslide susceptibility in the Rif, North of Morocco compared to the logistic regression (LR). Similarly, landslide susceptibility maps were produced by using multilayer perceptron (MLP) and ANN methods in the Mediterranean Rif coastal zone of Morocco (Harmouzi et al. 2019). It can be noted, however, that there is a considerable research gap in assessing landslide susceptibility using the integration between AIS and GIS in Morocco. On the other hand, this study is the first comparative evaluation between SVM, RBFN, and WoE models at the national level, thus improving the quality of demarcation of potential landslide areas in an area scarce with geographical data like the study area. Moreover, addressing the landslide susceptibility mapping performance using SVM algorithm represents the first contribution to the Moroccan context.

Study area

The N'fis basin is located in the centre of the Western High Atlas of Morocco. It is a mountainous area characterized by slope instability due to climatic, geological, and geomorphological features. Landslide incidents are the most prominent patterns of slope instability in the study area, which cause a threat to the life of the population, infrastructure, and spatial development. Thus, it is important to construct a reliable spatial prediction of landslide susceptibility within the framework of a safe and sustainable spatial planning process. Geographically, the N'fis basin extends between 7°55' W and 8°40' W longitude, and 30°52' N and 31°25' N latitude, with an area of approximately 1712 km^2. Geologically, the N'fis watershed is part of the High Atlas of Marrakech. It includes several lithological facies that range from Palaeozoic to Quaternary (Michard et al. 2008). The southern margin is dominated by primary age rock, primarily shales linked with limestone bars, magmatic rock, Permo-Triassic sandstones, and clays (Hollard et al. 1985). The mechanical and chemical alteration of these hard formations relatively allows the development of very slim skeletal soils and zonal brown soils.

The northern part of the study area is made up of limestone and marl from the Upper Cretaceous and Plio-Quaternary periods (Fig. 1). The N'fis river originates in the southwestern part of the Atlas Mountains and flows northward over a length of 80 km passing along several villages. The altitude ranges from 641 to 4164 m.a.s.l, with an average altitude and slope of 1860 m and 22 degrees, respectively. The climatic features in the study basin is arid to semi-arid, with an annual average temperature of roughly 18.6 °C, a maximum of 47.5 °C in July, and a minimum of 7.5 °C in January. However, the annual precipitation is 375 mm. March and April are the highest monthly rainfall, while July and August are the lowest.

Material and methodology

The process of landslides susceptibility mapping in the study area included the following stages: (a) digitizing the current landslide events and division into training and test datasets, (b) mapping the causative factors layers, (c) mapping landslide susceptibility using spatial calibration between training dataset and driving factors using SVM, RBFN, and WoE models, and d) evaluation of accuracy mapping using the test dataset. However, Fig. 2 shows the flowchart implemented in this study.

Landslide inventory map

Mapping the spatial distribution of historical landslide events is considered a critical step in forecasting landslide-prone zones (Carrara et al. 1995; Abdo et al., 2022). Many significant features, however, can be extracted from inventory map, like sites of current landslide events, landslides pattern, and motivations of landslides (Tien Bui et al. 2019). Inventorization of landslides is a systematic evaluation of the current distribution, extent, types, and patterns of landslides in the area under investigation using related methods (Tseng et al. 2015; Manchar et al. 2018). Based on fieldwork and interpretation of Google Earth satellite images, 156 landslide events were determined in order to construct the landslide inventory map in the N'fis basin. In this study, the landslide inventory map was constructed using the random sampling method (RSM) (Hong et al. 2018). A percentage of 70% of landslides were randomly determined as a training dataset, while the rest of the percentage (30%) were used for the model validation goals. These ratios are the most commonly used in the recent literature (Pourghasemi and Rahmati 2018; Wang et al. 2020a, b) (Fig. 3).

Predisposing factors

In this assessment, fourteen causative factors were selected to map the landslide susceptibility in the study

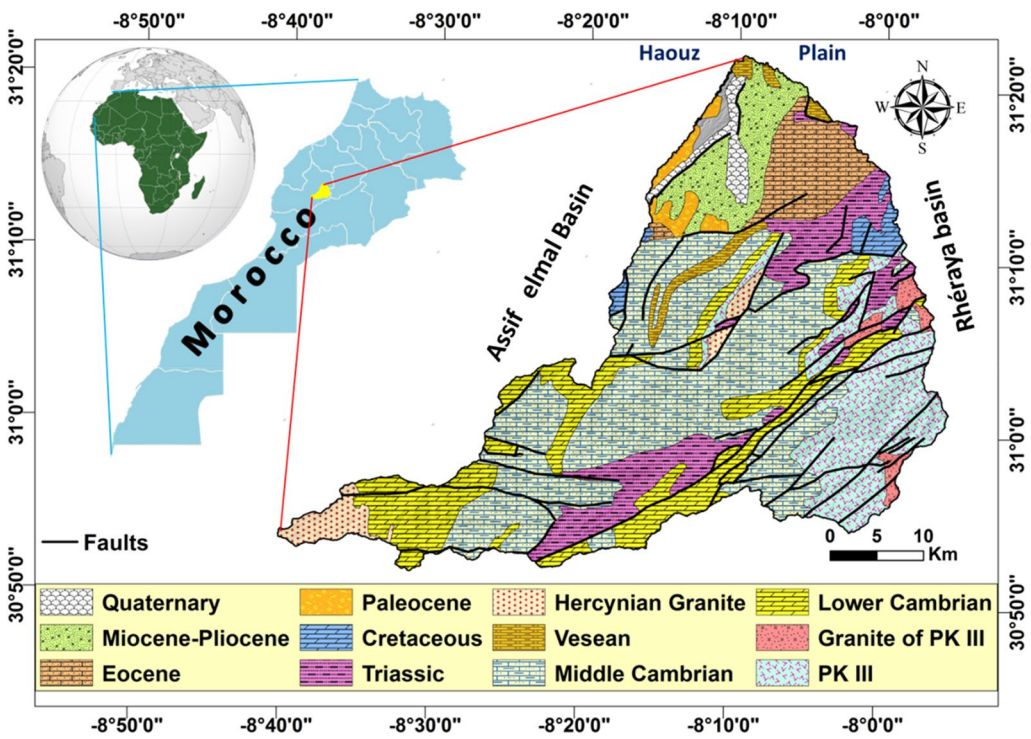

Fig. 1 Geographical location of the N'fis basin

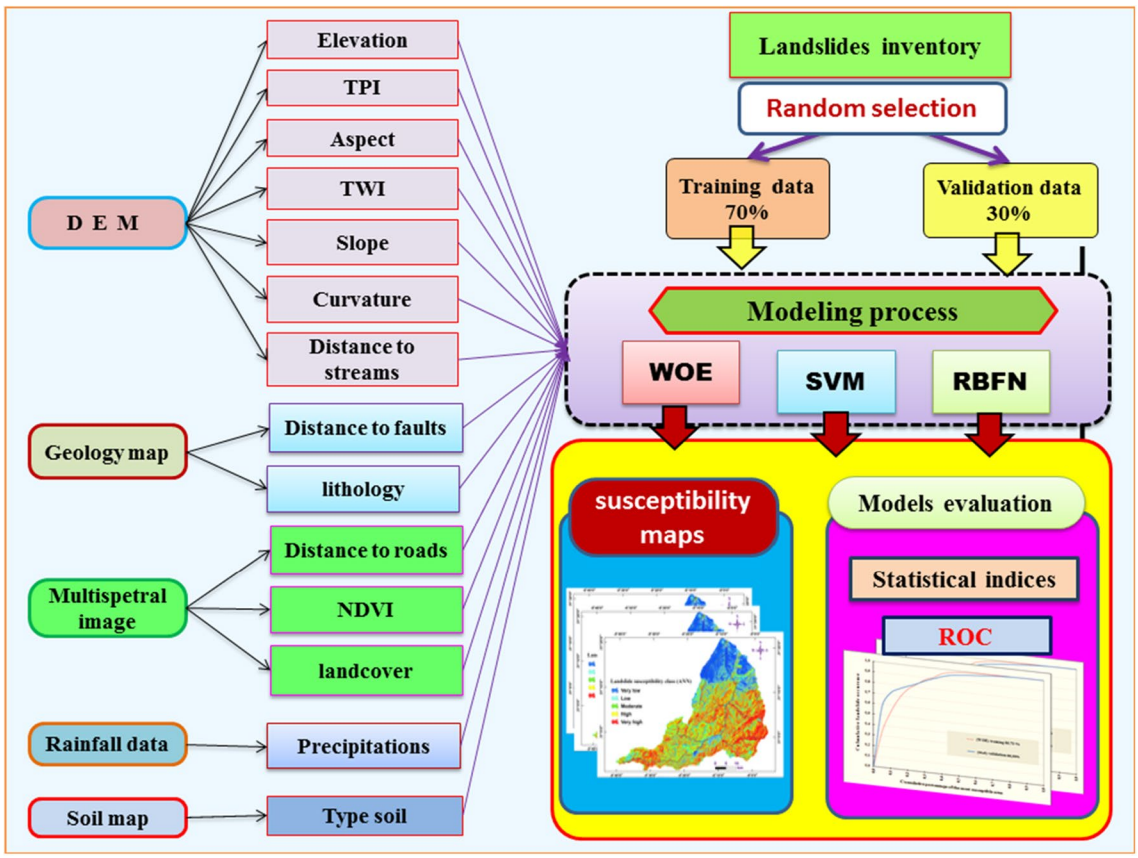

Fig. 2 Flowchart of the developed methodology

area, including slope, aspect, elevation, topographic wetness index (TWI), topographic position index (TPI), curvature, distance to rivers, distance to roads, Normalized Difference Vegetation Index (NDVI), Land use/Land cover (LULC), soil type, lithology, and rainfall. The thematic maps of the different geomorphological factors were produced using several using a digital elevation model (DEM) with a spatial resolution of 12.5 m. This DEM is provided by ALOS PALSAR. The ALOS mission was initiated on January 24, 2006, and ended operations on April 22, 2011. The Japanese government approved the ALOS mission, with the overarching goal of ensuring the continuation of data utilized for regional observation and environmental monitoring. The PALSAR sensor is one of ALOS' three devices (Wang et al. 2020a, b; Jaafari et al. 2022a, b; Abdo HG 2020; Nasir et al. 2022). In addition, the geological map of Morocco has been used to construct the distance to fault and lithologic maps. NDVI and the LULC maps were produced based on multispectral images (sentinel 2). However, the soil map was obtained by referring to the works of Mtaiau (2002) (Table. 1). All of the aforementioned parameters were combined in a GIS-based system and saved in a raster grid format with a resolution of 12.5/12.5 m (Fig. 4).

Landslide causatives factors importance

The evaluation of the significance of the predisposing factors is one of the objective procedures in the studies of mapping landslides susceptibility as a result of the restriction of the mutual influence of those factors in creating the state of landslide (Pham et al. 2018; Hosseinalizadeh et al. 2019). In the present study, the Information gain ratio (IGR) method was adopted to assess the contribution of different factors to landslide occurrence. Increasing the IGR values indicates the significant influence of the factor for the landslide model, and vice versa.

Landslide susceptibility indicators

Weights of evidence (WoE)

The WoE technique is a bivariate method that takes many variables into consideration and is typically used to estimate the landslide event occurrence based on the training dataset (Song et al. 2008). Many landslide scholars

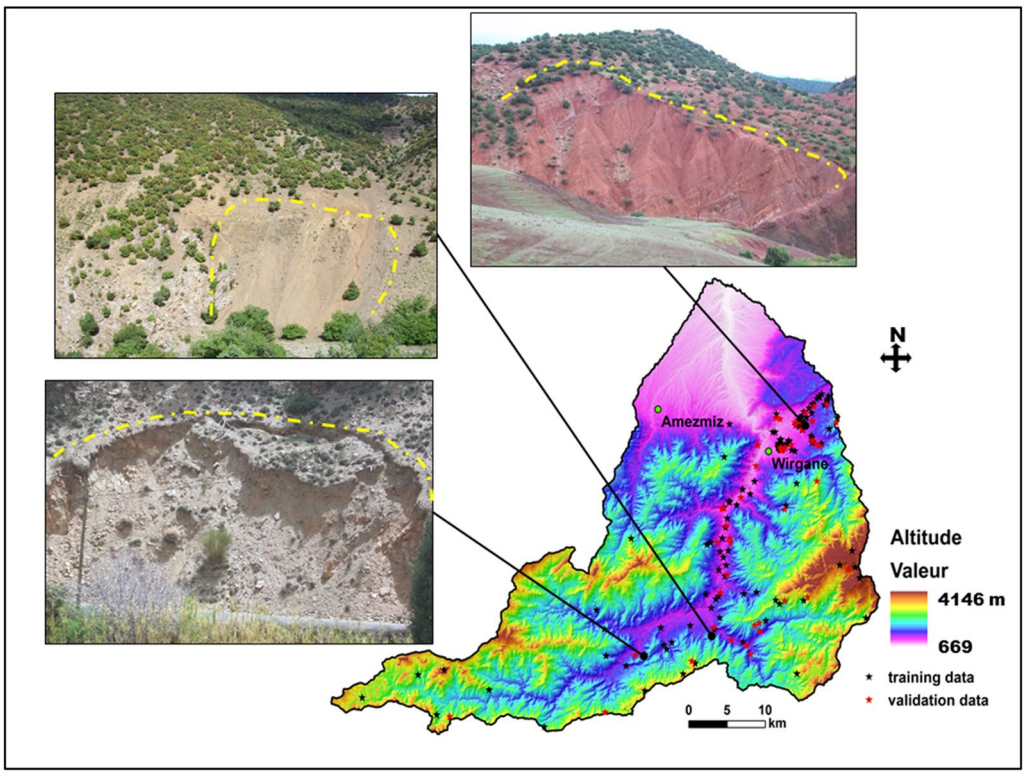

Fig. 3 Inventory map and examples of landslides in the N'fis basin

Table 1 Data sources used in the current study

Factors	Data source		Resolution/Scale	Date of acquisition
Elevation, Slope angle, Distance to stream, Distance to faults, TWI, TPI, Curvature, Slope aspect	DEM downloaded from: https://vertex.daac.asf.alaska.edu		12.5 m	2018
Distance to roads, NDVI, LULC	Satellite images downloaded from the site: https://scihub.copernicus.eu	B02 - B03 B04 - B08	10 m	2019
		B05 - B06 - B07 B12 - B08A—B11	20 m	
		B01 - B09 - B10	60 m	
Soil type	Soil map (Mathieu 2002)			2002
Lithology	Geologic map (Marrakech 1/500000)		1/500000	
Rainfall	Rainfall data (Tensift Basin Hydraulic Agency)		–	2018

have commonly devoted WoE method to landslide susceptibility mapping (Batar and Watanabe 2021; Kontoes et al. 2021). Moreover, it is a data-driven strategy that employs a log-linear variation of Bayesian analysis. The WoE technique is established on the basis that future landslide events will take place under impacts similar to those contributing to prior landslides.

When an adequate training dataset inventory is available, WoE uses prior and posterior (predicted) probability to evaluate the relative relevance of evidentiary elements. WoE method is applied by calculating two basic parameters: negative weight (W^-) and positive weight (W^+). Each landslide causative factor (B) is weighted according to the presence or absence of the landslide events locations (A) using Eqs. 1 and 2 (Bonham-Carter 1991):

$$W^+ = ln\frac{P\{B/A\}}{P\{B/\overline{A}\}}, \tag{1}$$

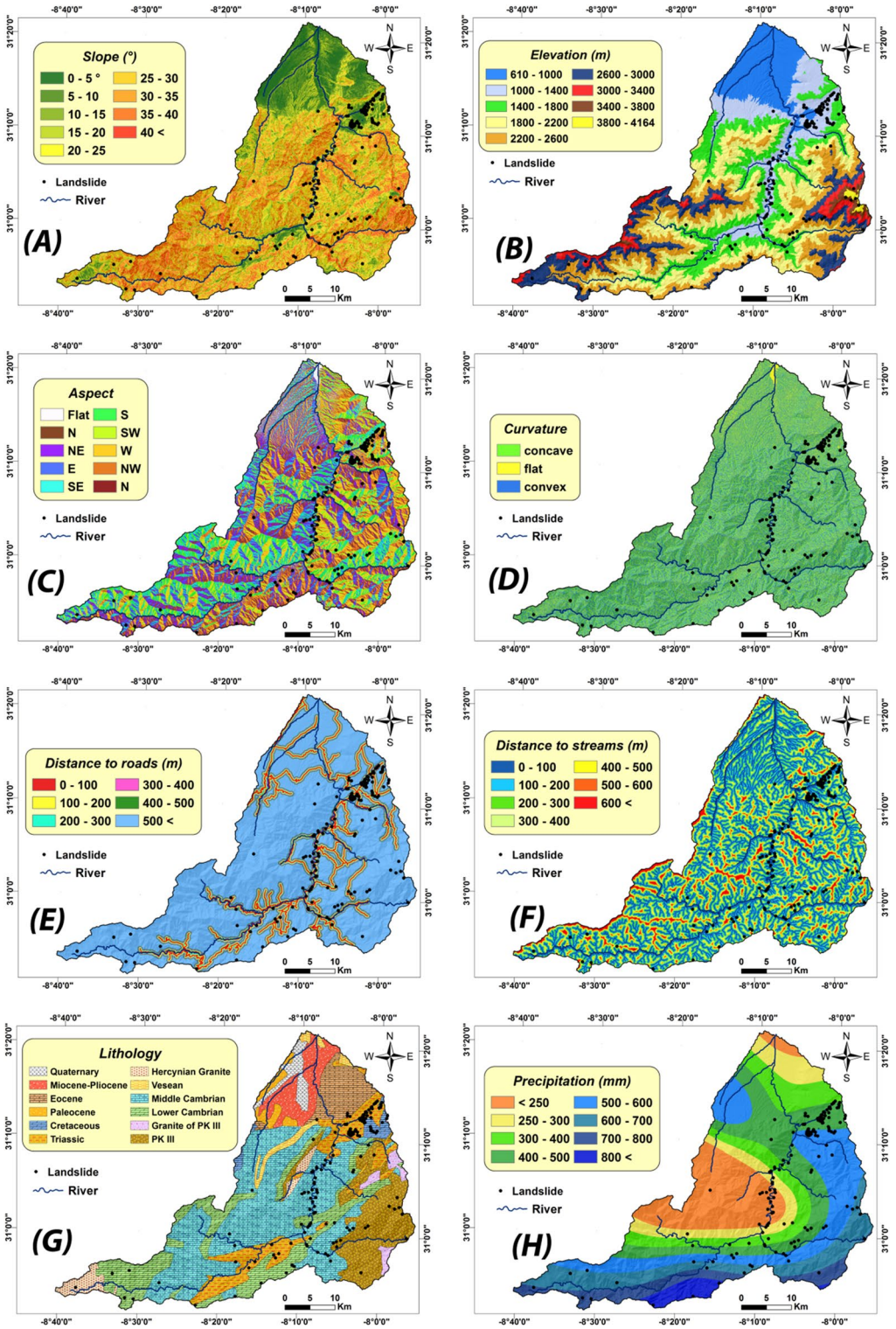

Fig. 4 Landslide conditioning factor **A** slope, **B** elevation, **C** aspect, **D** curvature, **E** distance to roads, **F** distance to rivers, **G** lithology, **H** rainfall, **I** NDVI, **J** land use, **K** distance to faults **L** TWI, **M** soil type, **N** TPI

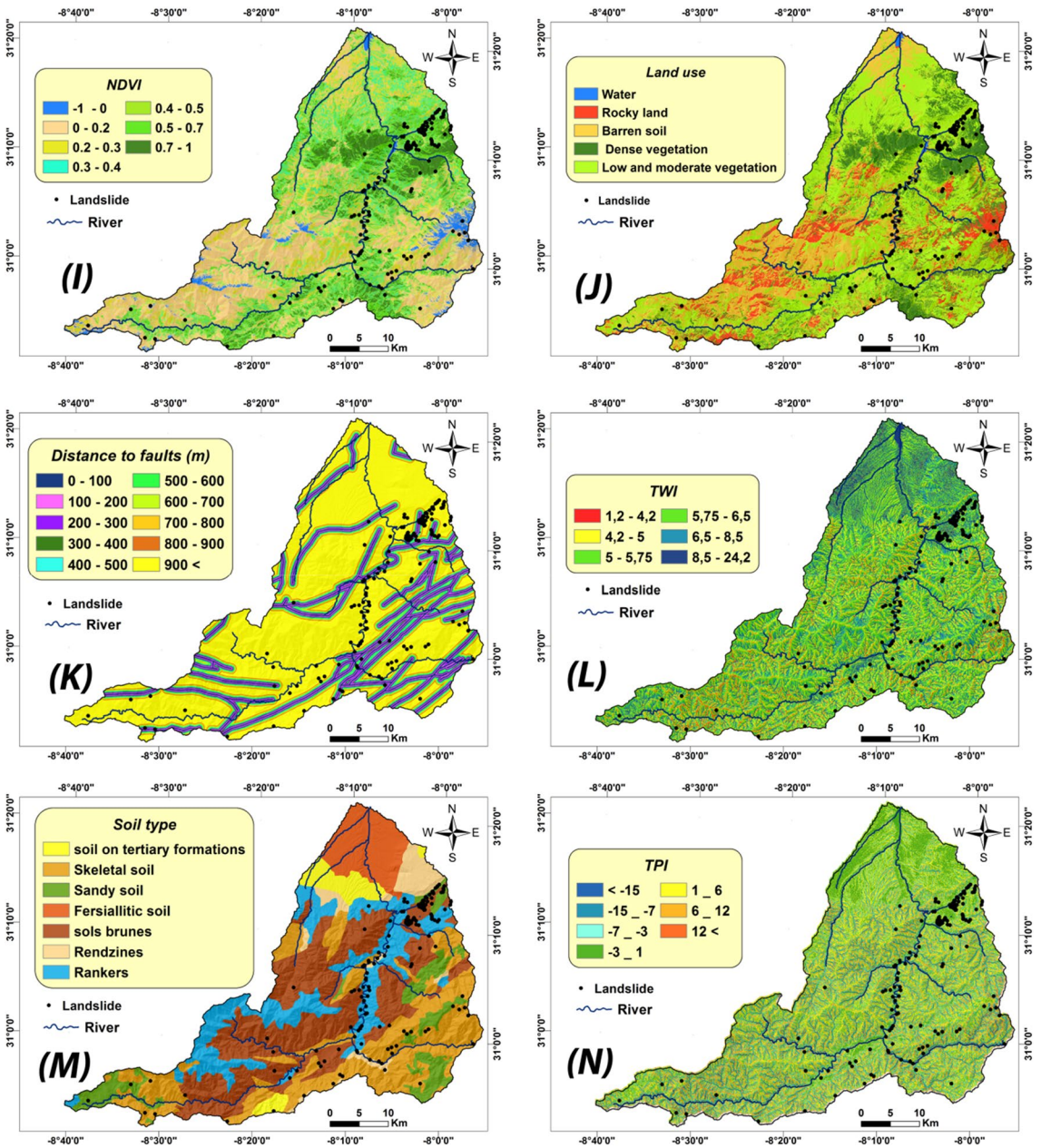

Fig. 4 continued

$$W^{-} = ln\frac{P\{\overline{B}/A\}}{P\{\overline{B}/\overline{A}\}}, \tag{2}$$

where P is the probability of the percentage, ln is the natural logarithm, W- is the negative weight, and $W+$ is the positive weight. $(\overline{B})$ is the absence of the landslide causative factor, (B) is the presence of the landslide causative factor, (A) is the absence of the landslide event location, and A is the presence of the landslide event location (Chen et al. 2016). In this sense, a positive weight indicates the presence of a landslide-causing factor, and its size indicates a favourable spatial correlation between these two inputs. However, a negative weight denotes a negative spatial association and the lack of the landslide causative factor at the landslide site.

Support vector machine (SVM)

The support vector machine (SVM) is considered among the novel machine learning algorithms (MLA) proposed by Vapnik (1995). SVM relies on non-linear transformations of variables in higher dimensional feature space (Oh and Pradhan 2011; Tien Bui et al. 2018; Yousefi et al. 2022). SVM is an accurate simulation method used for classification and regression based on statistical learning theory (Hong et al. 2017). In the first step of application, like most MLAT models, SVM must be learned by a training dataset, then the trained model will be used to assess the issue of the test dataset (Brenning 2005). Two key concepts perform as the foundation of the SVM approach, which handles discriminative issues. The first one is a hyperplane for optimum linear separation that divides the data models. The second one involves transforming the original non-linear data models using kernel functions into the most suitable data model (Yao et al. 2008). The set of separable linear training vectors xi (i = 1, 2,..., *n*) with two classes, represented by yi = ± 1, is needed for the two-class SVM model. The SVM goal is to find an n-dimensional hyperplane that discriminates between the two classes. The two classes are separated in n dimensions by the largest deviation that can be mathematically reduced using Eq. 3 (Yilmaz 2009):

$$\frac{1}{2}\|w\|^2 \tag{3}$$

with the following condition:

$$y_i((w.x_i) + b) \geq 1, \tag{4}$$

where w is the normal separator hyperplane, b is a scalable datum, and (.) signifies a multiplication operation. The following is obtained using Lagrangian coefficients of cost:

$$L = \frac{1}{2}\|W\|^2 - \sum_{i=1}^{n} \lambda_i \big(y_i((wx_i) + b) - 1\big), \tag{5}$$

where λ_i is the Lagrangian multiplier. Equation 6 can be minimized by using the w and b ratios as a standard. A variable ξ_i can be used as a weak meaning (slack variables ξ_i), in which case Eq. 7 becomes

$$y_i((w.x_i) + b) \geq 1 - \xi_i, \tag{5}$$

$$L = \frac{1}{2}\|W\|^2 - \frac{1}{\upsilon n}\sum_{i=1}^{n} \xi_i. \tag{6}$$

Radial basis function network (RBF)

The radial basis function (RBF) is a receptive-field neural network model that is applied to deal with multivariate interpolation problems (He et al. 2019). Subsequently, RBF technique has been used in landslide detection over many areas (Powell 1992; Zeybek and Şanlıoğlu 2020). A K-means clustering algorithm is the basis of the RBF network model. It is efficient in solving non-linear problems (Rumellhart 1986). The principle of RBF model is relatively simple, fundamentally based on a radial function. Initially, it imports the data into the input layer without any computation. Then, it processes the non-linear problem of the hidden layer neuron, and finally, it sends the results to the linear output layer. The RBF network is characterized by a single hidden layer, but there is no hidden layer in the model. The activation function in the hidden layer can be as follows: *f*: Rn → R, if the model is well trained. The basic function commonly used by researchers in RBF networks is the Gaussian one, which can be written as (Lei et al. 2020)

$$fi(\mathrm{x}) = fi\left(e^{\frac{-\|xp-ci\|}{di}}\right), i = 1, 2, \ldots., n, \tag{7}$$

$$Y = W^t f_p, \tag{8}$$

where $C_i \in$ Rn indicates the centre of the basis function. f_i $d_i \in$ R is the radius of the first hidden layer node. f_p is the hidden node vector.

Validation of landslide susceptibility maps

Statistical validation is employed to assess and compare the implementation and quality of performance of machine learning algorithms in mapping landslide susceptibility. In the current evaluation, the receiver operating characteristics (ROC) curve with the area under curve (AUC) was developed to assess the performance of the three models used and to validate the generated landslide susceptibility maps. On the x-axis is the false-positive rate (specificity), while on the y-axis is the real positive rate (sensitivity). Furthermore, the performance of the modelling techniques used was evaluated using some statistical measures. Each model probability was compared to historical landslide locations to create a confusion matrix that yields true negative (TN), true positive (TP), false negative (FN), and false positive (FP) (Park et al. 2019):

$$Specifity = \frac{TN}{FP + TN}, \tag{9}$$

$$Sensitivity = \frac{TP}{FN + TP}, \tag{10}$$

$$Accuracy = \frac{TN + TP}{FP + TP + FN + TN}, \tag{11}$$

$$Precision = \frac{TP}{FP + TP}. \quad (12)$$

Results and analysis

Assessment of landslide causatives factors importance

The IG approach was employed to assess the quantitative impact of each landslide conditioning factor in the creation of landslide events. However, the removal of conditioning factors with zero predictive value is recommended by Chen et al. (2017). All fourteen landslide factors showed positive predictive capacity ratings, as illustrated in Fig. 5. The slope has the highest predictive capability with average merit (AM) value of 0.098. However, the rest of conditioning factors have less predictive capabilities i.e. distance to roads (0.07), distance to rivers (0.069), lithology (0.054), altitude (0.051), precipitation (0.048), soil type (0.046), TWI (0.032), NDVI (0.029), aspect (0.018), TPI (0.016), curvature (0.009), LULC (0.005), and distance to faults (0.004). Additionally, AG analysis indicated that all motivation factors have a positive contribution, therefore can be included in the implemented landslide modelling.

Application of landslide susceptibility models

In the present study, two machine learning models (SVM and RBFN) and one bivariate statistical model (WoE) were applied to assess the landslide susceptibility at the N'fis watershed. After testing the importance of the variables by the IG method, fourteen causative factors were used as inputs to the landslide modelling process. The outcomes of the WoE analysis, however, are shown in Table 2. The spatial correlation between landslide events and each class of causative factors was measured using the contrast values (*C*). High values of *C* indicate a positive effect between the class of each factor and the occurrence of landslides. The landslide susceptibility value obtained using the WoE model ranges from 0.014 to 0.978, which was reclassified into five classes using the *Natural Breaks* method in ArcGIS 10.4: very low (0.014–0.195), low (0.195–0.334), moderate (0.334–0.516), high (0.516–0.679), and very high (0.679–0.978) as shown in Fig. 6.

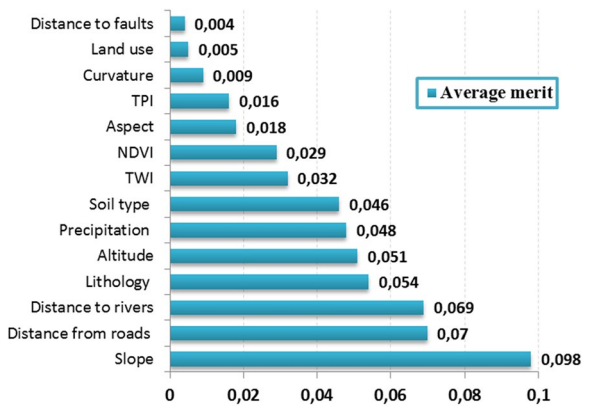

Fig. 5 Predictive capabilities of the fourteen landslide conditioning factors

TensorFlow was used in this assessment to build the SVM model. SVM ideal parameters were determined through a number of trial and error procedures. However, the degree is 3, the gamma is the reciprocal of the number of features, the kernel function coefficient is 0.5, and the polynomial kernel function was chosen as the kernel function. The computed LSI values using the SVM model ranged from 0.013 to 0.987. The landslide susceptibility map was created by converting these values into a raster format in the GIS environment as Fig. 7 shows. The landslide susceptibility map was categorized into five categories of SVM model ranging: very high (0.755–0.987), high (0.630–0.755), moderate (0.378–0.630), low (0.235–0.378), and very low (0.013–0.235). Using the *Natural Break* method in GIS, the spatial zone of very high, high, medium, low, and very low susceptibility assigned as 7.69%, 17.18%, 29.48%, 25.75%, and 19.9%, respectively.

The RBFN model was built using the landslide training dataset. The Weka software ten− fold cross− validation procedure not only decreases model variability but also eliminates the problem of overfitting throughout the modelling process as suggested by several studies (Wang et al. 2020a, b). The parameters used in the RBFN model are as follows: the clustering seed is 1, the maximum number of iterations is − 1, the number of clusters is 2, the minimum standard deviation is 0.1, and the ridge is 1.0E− 8. The landslide susceptibility index values calculated by the RBFN model ranged from 0.015 to 0.971. These values were reclassified into five classes: very high (0.638–0.932), high (0.434–0.638), moderate (0.252–0.434), low (0.110–0.252), and very low (0.005–0.110) based on the Natural Breaks method. The very low class has the largest area (11.58%), followed by low (24.36%), moderate (31.14%), high (22.87%), and very high (10.05%) as Fig. 8 depicts. Figure 9, in this context, shows graphically the proportional distribution of the susceptibility classes obtained by the three models applied in this assessment.

Further, the visual analysis revealed similar spatial distributions of landslide susceptibility classes in the three maps produced in this evaluation. The southeastern part of the study area shows a very high susceptibility to landslides. The areas along with the rivers in most parts of the N'fis basin are also vulnerable to landslides. These maps also show a low to very low susceptibility to landslides in

Table 2 WoE weights for the different classes of each parameter based on landslide occurrences

Factor	Class	Number of pixels in class	Percentage of domain (PD)	Number of landslide pixels	Percentage of landslide (PL)	*W*+	*W*−	*C*
Elevation	669–1000	1,272,189	11,609	330	0.485	− 1.381	0.052	− 1.433
	1000–1400	1,456,731	13,294	16,076	23,640	0.251	− 0.055	0.307
	1400–1800	1,969,797	17,976	7769	11,425	− 0.198	0.034	− 0.232
	1800–2200	2,492,537	22,746	8532	12,547	− 0.260	0.054	− 0.314
	2200–2600	1,904,152	17,377	12,212	17,958	0.014	− 0.003	0.017
	2600–3000	1,283,162	11,710	10,039	14,763	0.101	− 0.015	0.116
	3000–3400	411,264	3753	5285	7772	0.319	− 0.019	0.337
	3400–3800	128,853	1176	5094	7491	0.819	− 0.029	0.848
	3800–4146	39,502	0360	2665	3919	1.064	− 0.016	1.080
Aspect	Flat	238,676	2178	424	0.624	− 0.545	0.007	− 0.552
	North	685,146	6252	5883	8651	0.742	− 0.011	0.753
	Northeast	1,311,145	11,965	6248	9188	− 0.116	0.014	− 0.129
	East	1,142,489	10,426	3563	5240	− 0.300	0.025	− 0.325
	Southeast	1,374,238	12,541	5514	8109	− 0.191	0.022	− 0.212
	South	1,270,892	11,598	7680	11,294	− 0.012	0.002	− 0.013
	Southwest	1,249,359	11,401	6615	9728	− 0.070	0.008	− 0.078
	West	1,363,696	12,445	10,578	15,555	0.697	− 0.016	0.713
	Northwest	1,612,963	14,719	14,325	21,066	0.556	− 0.034	0.590
Slope	0–5	877,640	8009	283	0.416	− 1.287	0.035	− 1.322
	5–10	949,345	8663	773	1137	− 0.884	0.035	− 0.919
	10–15	924,563	8437	1879	2763	− 0.487	0.026	− 0.513
	15–20	1,223,898	11,169	4479	6587	− 0.231	0.022	− 0.253
	20–25	1,521,999	13,889	7442	10,944	− 0.104	0.015	− 0.119
	25–30	1,908,976	17,421	11,495	16,904	− 0.014	0.003	− 0.016
	30–35	1,750,461	15,974	14,846	21,832	0.236	− 0.031	0.268
	35–40	1,108,049	10,112	13,325	19,595	0.289	− 0.049	0.338
	40–80	693,256	6326	13,480	19,823	0.501	− 0.068	0.569
Distance to river	0–100	3,038,244	27,726	23,082	33,943	0.788	− 0.039	0.727
	100–200	2,629,077	23,992	17,277	25,407	0.024	− 0.008	0.032
	200–300	2,067,878	18,871	12,082	17,767	− 0.027	0.006	− 0.033
	300–400	1,480,579	13,511	8056	11,847	− 0.058	0.008	− 0.066
	400–500	930,448	8491	5441	8001	− 0.026	0.002	− 0.029
	500–600	494,119	4509	1766	2597	− 0.241	0.009	− 0.250
	> 600	317,842	2900	298	0.438	− 0.823	0.011	− 0.834
Distance to Faults	0–100	579,171	5285	2954	4344	− 0.086	0.004	− 0.090
	100–200	571,586	5216	2666	3920	− 0.125	0.006	− 0.131
	200–300	555,729	5071	2712	3988	− 0.105	0.005	− 0.110
	300–400	538,959	4918	3318	4879	− 0.004	0.000	− 0.004
	400–500	510,991	4663	4471	6575	0.150	− 0.009	0.159
	500–600	475,154	4336	4134	6079	0.148	− 0.008	0.156
	600–700	445,860	4069	3220	4735	0.066	− 0.003	0.069
	700–800	422,393	3855	3065	4507	0.068	− 0.003	0.071
	800–900	401,590	3665	2323	3416	− 0.031	0.001	− 0.032
	> 900	6,456,754	58,922	39,139	57,556	− 0.012	0.017	− 0.028

Table 2 (continued)

Factor	Class	Number of pixels in class	Percentage of domain (PD)	Number of landslide pixels	Percentage of landslide (PL)	*W*+	*W*−	*C*
NDVI	− 1.0	308,723	2817	8542	12,561	− 0.058	0.046	− 0.102
	0–0.2	3,585,799	32,723	27,524	40,475	0.592	− 0.053	0.645
	0.2–0.3	2,497,976	22,796	11,117	16,348	0.146	0.035	0.111
	0.3–0.4	1,397,659	12,754	5132	7547	− 0.229	0.025	− 0.255
	0.4–0.5	903,324	8243	3753	5519	− 0.175	0.013	− 0.188
	0.5–0.7	1,241,592	11,330	5496	8082	− 0.148	0.016	− 0.163
	0.7–1	1,023,114	9337	6438	9467	− 0.006	0.001	− 0.007
Curvature	concave	7,305,932	12,561	13,597	14,328	0.080	− 0.011	0.91
	flat	58,471,399	54,302	54,210	64,191	0.959	− 0.009	0.968
	convex	43,631,245	33,137	20,048	21,481	− 0.052	0.024	− 0.076
Lithology	Hercynian granite	291,252	2658	686	1009	− 0.422	0.007	− 0.430
	Lower Cambrian	1,805,221	16,474	16,978	24,967	0.181	− 0.047	0.228
	Granite PK III	161,417	1473	0	0.000	0.000	0.006	− 0.006
	PK III	1,487,143	13,571	21,237	31,230	0.365	− 0.100	0.464
	Triassic	1,184,184	10,806	7184	10,564	0.710	− 0.001	0.711
	Middle Cambrian	3,899,874	35,589	21,405	31,477	− 0.054	0.028	− 0.082
	Visean	205,846	1878	59	0.087	− 1.338	0.008	− 1.346
	Paleocene	147,493	1346	0	0.000	0.000	0.006	− 0.006
	Cretaceous	174,341	1591	415	0.610	− 0.418	0.004	− 0.422
	Eocene	663,642	6056	38	0.056	− 2.038	0.027	− 2.065
	Miocene–Pliocene	66,174	0,604	0	0.000	0.000	0.003	− 0.003
	Pliocene	29,686	0,271	0	0.000	0.000	0.001	− 0.001
	Quaternary	194,812	1778	0	0.000	0.000	0.008	− 0.008
	Miocene	647,102	5905	0	0.000	0.000	0.027	− 0.027
Distance to roads	0–100	721,332	6583	8055	11,845	0.257	− 0.025	0.282
	100–200	650,787	5939	5050	7426	0.098	− 0.007	0.105
	200–300	589,638	5381	3793	5578	0.016	− 0.001	0.016
	300–400	542,723	4953	3465	5095	0.012	− 0.001	0.013
	400–500	503,998	4599	3000	4412	− 0.018	0.001	− 0.019
	> 500	7,949,709	72,546	44,639	65,644	− 0.045	0.103	− 0.148
TPI	−97–15	171,619	1,566	2260	3323	0.330	‡0.008	0.338
	−15–7	1,205,423	11,000	11,019	16,204	0.169	− 0.026	0.195
	−7–− 3	1,723,329	15,726	13,873	20,401	0.113	− 0.025	0.138
	−3–1	3,223,516	29,417	15,204	22,358	− 0.120	0.042	− 0.162
	1–6	2,931,384	26,751	13,808	20,305	− 0.121	0.037	− 0.158
	6–12	1,320,244	12,048	8340	12,264	0.007	− 0.001	0.008
	12–104	382,672	3492	3498	5144	0.169	− 0.008	0.177
Soil	rankers	1,875,895	17,119	9891	14,545	− 0.072	0.013	− 0.085
	rendzine	498,491	4549	1617	2378	− 0.283	0.010	− 0.293
	Brown soil	3,526,990	32,186	16,797	24,701	− 0.116	0.046	− 0.162
	fersiallitic soil	892,431	8144	0	0.000	0.000	0.037	− 0.037
	sandy soil	879,257	8024	4396	6465	− 0.095	0.007	− 0.102
	skeletal soil	2,839,452	25,912	35,301	51,912	0.303	− 0.188	0.491
	soil on tertiary formations	445,671	4067	0	0,000	0.000	0.018	− 0.018

Table 2 (continued)

Factor	Class	Number of pixels in class	Percentage of domain (PD)	Number of landslide pixels	Percentage of landslide (PL)	*W*+	*W*−	*C*
TWI	< 4.20	582,243	5313	5073	7460	0.148	− 0.010	0.158
	4.2–5	2,333,240	21,292	14,498	21,320	0.000	0.000	0.000
	5–5.75	2,904,133	26,502	16,724	24,593	− 0.033	0.011	− 0.045
	5.75–6.5	2,027,508	18,502	12,200	17,941	− 0.014	0.003	− 0.017
	6.5–8.5	1,958,107	17,869	14,663	21,563	0.082	− 0.020	0.102
	8.5 <	1,152,956	10,521	4844	7123	0.370	− 0.016	− 0.386
LULC	water	24,042	0,219	0	0,000	0.000	0.001	− 0.001
	dense vegetation	1,964,037	17,923	14,840	21,823	0.085	− 0.021	− 0.106
	medium to low vegetation	5,461,797	49,842	24,228	35,628	− 0.148	0.110	− 0.258
	stony ground	1,326,975	12,109	20,785	30,565	0.405	− 0.103	0.508
	bare earth	2,181,336	19,906	8140	11,970	0.223	− 0.041	0.264
Precipitation	< 300	569,470	5197	6329	9307	0.255	− 0.019	− 0.274
	300–350	1,222,198	11,153	8588	12,629	0.054	− 0.007	− 0.061
	350–400	2,418,710	22,072	17,731	26,074	0.072	− 0.023	0.095
	400–450	2,771,891	25,295	15,085	22,183	− 0.058	0.018	− 0.076
	450–500	984,840	8987	3193	4695	0.283	− 0.020	0.303
	500–550	447,141	4080	7116	10,464	0.413	− 0.030	0.443
	550–600	775,859	7080	1348	1982	0.555	− 0.023	0.578
	> 600	1,768,078	16,135	8612	12,664	0.706	− 0.018	0.724

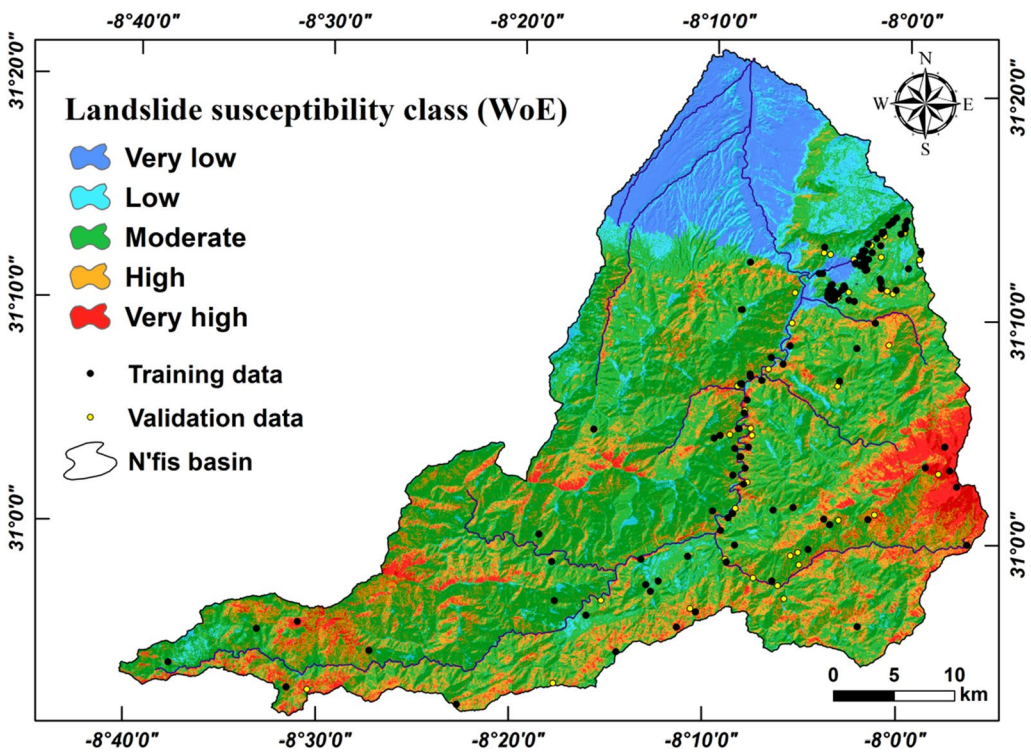

Fig. 6 Landslide susceptibility map using WoE model

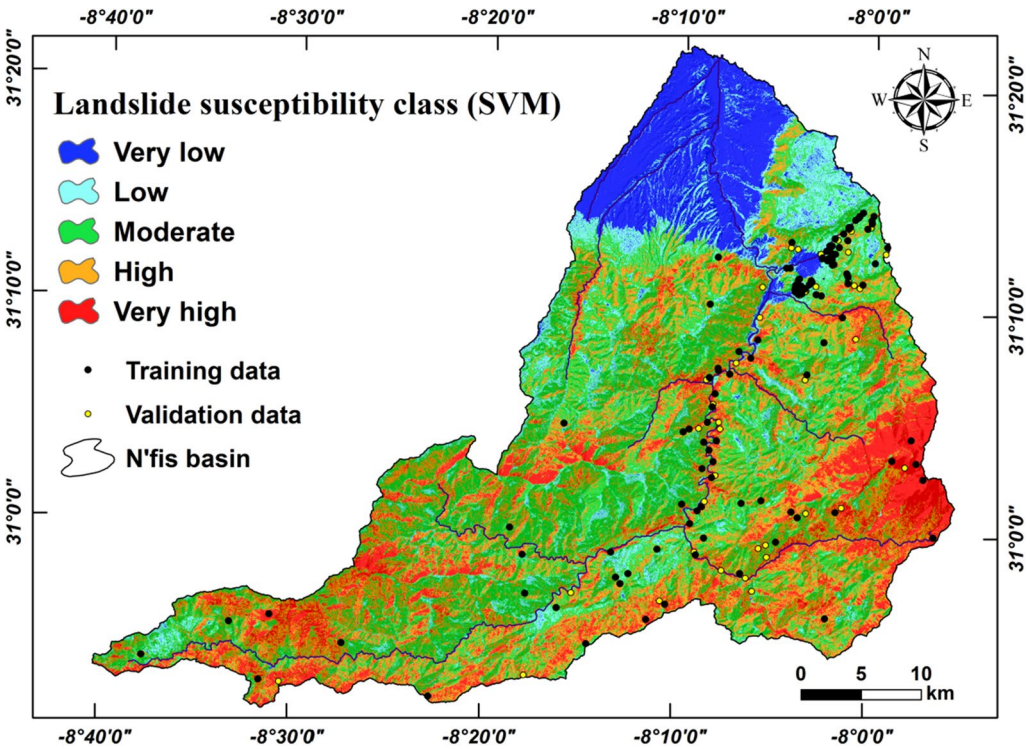

Fig. 7 Landslide susceptibility map using SVM model

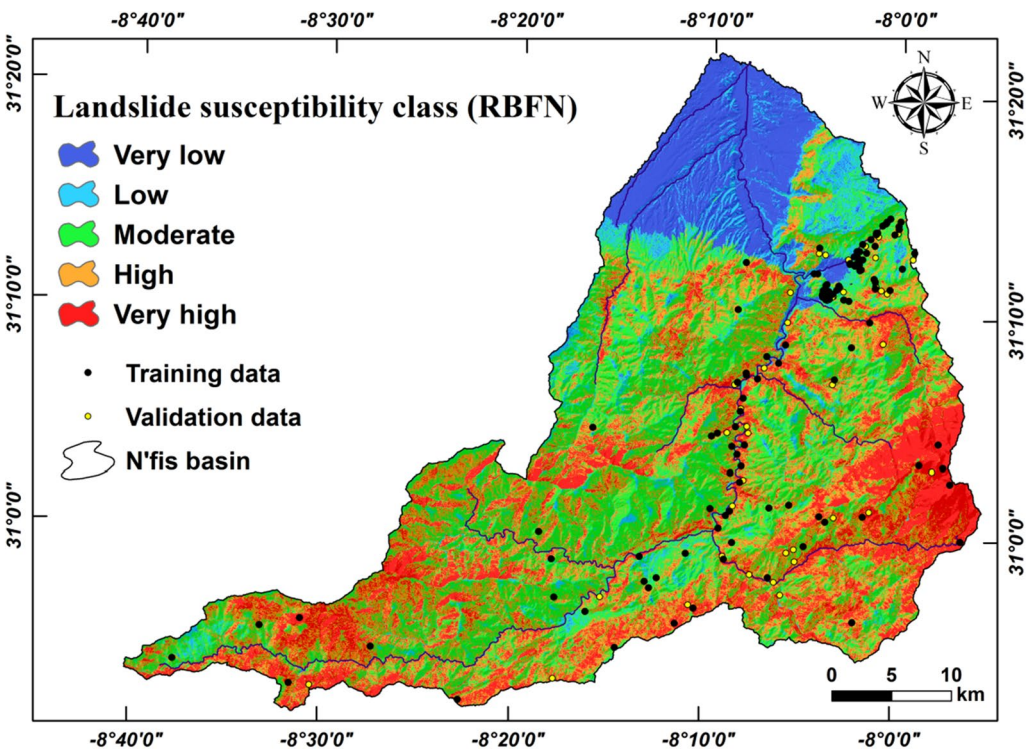

Fig. 8 Landslide susceptibility map using RBFN model

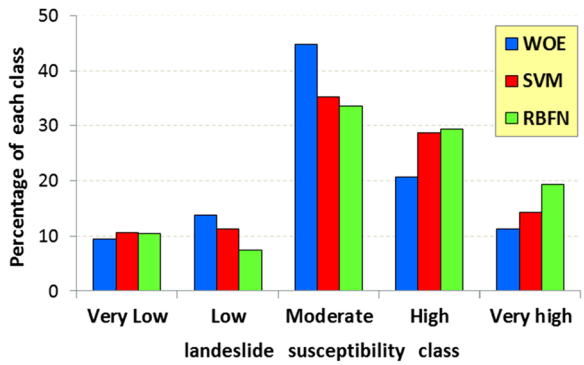

Fig. 9 Distribution of landslides in each landslide susceptibility category

the northern part of the basin featured by gentle slopes. These results highlight the importance of the slope and distance to the river factors in the creation of landslide events which corresponds to the GI method outcome.

Validation and comparison of the models

The quantitative measurement of the accuracy of landslide susceptibility maps produced by the different classification models is a fundamental step (Luo et al. 2018). Moreover, the resulting landslide susceptibility maps will have no practical significance without validation of a landslide susceptibility model (Pham et al. 2017a, b). For this reason, the ROC and other statistical indices were used to evaluate the predictive performance of the models applied in this study. Using the training dataset, the AUC values for the WoE, SVM, and RBFN models were 83.72%, 94.37%, and 93.68%, respectively. The same ranking was obtained using the validation data with a little increase in the AUC values. In fact, the SVM model still has the best performance (94.60%), followed by RBFN (93.30%), and finally WoE (87.68%) (Fig. 10). However, the landslide susceptibility map developed with the SVM model is the best performing one followed by the map produced by the RBF model, while the WoE model is the least performing.

The performance of the three models was also evaluated using several statistical indices (Table 3). The SVM model has the best performance, with the highest values of sensitivity (0.999), specificity (0.990), precision (0.997), and accuracy (0.987). With the RBFN model, we obtained a slightly lower performance than the SVM model. In

Table 3 Statistical indices of different prediction models

		Sensitivity	Specificity	Precision	Accuracy
Training data	WoE	0,660	0,927	0,815	0,839
	SVM	0,996	0,973	0,992	0,990
	RBFN	0,990	0,916	0,981	0,976
Validation data	WoE	0,706	0,916	0,829	0,839
	SVM	0,996	0,937	0,982	0,983
	RBFN	0,980	0,921	0,972	0,965

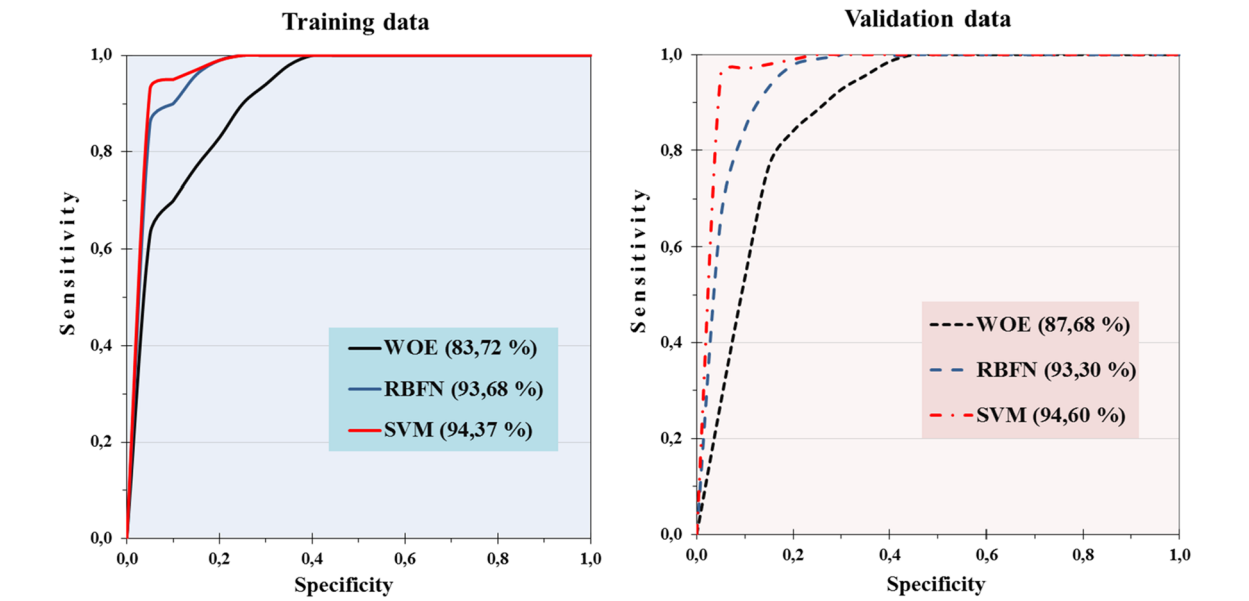

Fig. 10 Analysis of the ROC curve of different landslide models using training and validation dataset

this assessment, the WoE model is the least performing model with the lowest values of statistical performance indices.

Discussion

In Morocco, the landslides incidence is accelerating in mountainous areas due to the complex spatial integration of climate change, LULC change, and the pressure of human activities (El Hamdouni et al. 2022). Hence, there is an urgent need to conduct more accurate studies assessing landslide susceptibility with enhanced spatial outcomes. This accuracy is based on criteria of adequate data quality, appropriate modelling methods, and effective causative factors (Ayalew et al., 2005). In this study, a comparison performance of the WoE, RBFN, and SVM models was constructed in delineating the spatial susceptibility of landslides in N'fis basin with a total of 156 landslide events.

Evaluation of the correlation between historical landslide events and causal factors is a crucial step in landslide susceptibility modelling. This procedure is used to select the appropriate factors, thus improving the performance of the models used. In the current study, IG analysis was used to enhance the modelling process. With fourteen factors considered as motivating factors for landslides, the results of the IG analysis indicated that the slope, distance to road, and distance to river factors were the most important in creating landslide status with AM values of 0.098, 0.07, and 0.069, respectively. These results are consistent with the studies of Yu et al. (2019), Zhang et al. (2019), and Abedini et al., (2018). This can be justified by the intense mountainous geomorphological characteristics of the study area with an elevation of more than 4000 m.a.s.l. Steep slopes, which reach many locations more than 40 degrees, increase the potential landslide occurrences. Despite the importance of physical factors in creating the current stability of slope materials, landslide events are closely linked with human and economic factors that are very important in mountain watersheds (Lei et al. 2020; Saha et al. 2021).

One of the bivariate model merits is its flexible application because there is no need for training and parameter modification (Magliulo et al. 2009; Chen et al. 2020). In this evaluation, the SVM model achieved the best performance in producing a spatial susceptibility landslide map. In this regard, despite the flexibility of using bivariate statistics models, the machine learning algorithms provide the best performance due to the possibility of determining the best parameters involved in the modelling process, analysing the relationship between the driving factors and removing variance from the training dataset (Abedini et al. 2019a, b). Thus, the SVM model provided a reliable performance with a high accuracy rate that allowed us to reduce the limitations of this study. These investigations reveal that the occurrence of landslides is closely associated with geo− ecological factors (Huang et al. 2022). Moreover, the application of machine learning models, such as SVM and RBFN in this study, is relatively complex and requires data transformation. Despite this complexity, these models are recommended for assessing landslide susceptibility due to their high accuracy compared to the bivariate statistical model (Chen et al. 2020).

In this regard, the indicators of evaluating accuracy and performance proved the high potential of the three methods in mapping the landslide susceptibility in the study area. Despite this, those indicators reported that the SVM model was the most high quality in comparison to the WOE and RBFN model. Furthermore, many landslide susceptibility scholars have confirmed the high efficiency of the SVM model in evaluating landslides. Abedini et al. (2019a, b) reported that the SVM was more precise than the other models. Similarly, Tien Bui et al. (2012) stated that the SVM model outperformed landslide risk assessment compared to decision tree (DT) and Naïve Bayes (NB) algorithms. The same result was found in a study conducted by Ballabio and Sterlacchini (2012).

SVM has the merit of having non-linear kernel functions which deal with the non-linear association between landslide events and causative factors (Zhao and Zhao 2021). Furthermore, the SVM model application provided an optimal level of landslide vulnerability classification due to the ability to accurately separate the training dataset points of landslides and non-landslides (Kong et al., 2021). The RBFN has the features of unique global approximation, linear association of output significances in the network structure, reasonable classification capacity, and quick training rate (Kim et al. 2019). However, WoE provided an acceptable performance in mapping landslide susceptibility despite the collinearity between motivating factors and landslide events that affected the model performance. However, the three models showed remarkable consistency in the predictive ability of the training dataset and that of the verification dataset, which indicates that these models have achieved practical and reliable spatial results in mapping landslide susceptibility in the study area.

The three models applied confirmed that the eastern and southeastern regions were the most vulnerable to landslide events. However, this result is consistent with the observations of the extensive fieldwork carried out in the study area. In this respect, these areas are characterized by extreme elevation (< 4000 m), steep slopes (< 40°), intense rainfall storms, low vegetation density, fragile rock formations, dense fissures and faults, and rapidly topsoil eroding. These characteristics make these areas

highly prone to landslides, therefore should be included in mitigation and maintenance priorities (Mohammed et al. 2020).

In this regard, the diversity of data sources and the spatial resolution of the variables are the main certain uncertainty and limitations of this study. For example, the data resolution of DEM, LULC, lithology, and soil types was not consistent (Table. 1). Several studies indicate that choosing the appropriate spatial resolution remains a challenge in the context of advances in landslide modelling studies (Wang and Brenning 2021; Huang et al. 2022). However, these limitations are common in areas with scarce geographical data, such as the study area. All the thematic layers were resampled at a 12.5 m resolution in order to conduct this study. The absence of data of some important parameters, such as soil texture, soil depth, and water table depth, remains also among the main limitations of the current study. Despite these limitations and in light of the results of performance evaluation, the results of this study can be considered objectively efficient in improving the quality of spatial outputs related to landslide prediction at the national level.

Finally, the three implemented methods demonstrated sufficient performance for landslide susceptibility mapping. Nevertheless, the SVM model achieved suitable performance. Hence, it can be utilized to evaluate and create more reliable landslide susceptibility maps for appropriate landslide risk management. Overall, the outcomes of this study can introduce very valuable and critical knowledge for local decision-makers and LULC planners to mitigate and manage the high and very landslide susceptibility areas in the N'fis basin.

Conclusion

The identification of landslide-prone areas is an important procedure for LULC planning and developing landslide mitigation techniques. The aim of this study is to conduct a comparative evaluation of landslide susceptibility mapping using SVM, RBFN, and WoE models in the N'fis river basin, Morocco. An inventory map of 156 landslide events was produced and divided into 70% as a training dataset and 30% as a test dataset. Moreover, 14 causative factors, i.e. slope angle, elevation, slope aspect, LULC, TWI, curvature, lithology, distance to faults, distance to roads, TPI, rainfall, distance to rivers, NDVI, and soil type, were mapped using a different source database. These factors were spatially calibrated with the training dataset using the three models in order to map the landslide susceptibility in the study area.

The three maps produced were reclassified into five classes, i.e. very low, low, moderate, high, and very high. The high and very high areas are located in the eastern and southeastern parts of the basin, characterized by high altitudes and steep slopes. The maps obtained were validated by ROC and statistical indices, which showed that the SVM method is the most suitable performing (AUC = 94.60%), followed by RBFN (AUC = 93.30%), while the WoE model remains the least performing (AUC = 87.68%). The findings of this study showed that machine learning methods, such as SVM and RBFN, have improved the simulation maps of landslide susceptibility at the national level.

Acknowledgements
The authors are thankful to the editors and reviewers

Author contributions
HAN, HGA, II, and MN contributed to methodology and software; II, HAN, MN, and HA conducted formal analysis and investigation. MN, II, HAN, and HGA contributed to visualization; HAN, HA, MN, MAM, AAA, HGA, and HA were involved in writing—original draft preparation; HGA, HAN, II, MN, HA, AAA, and MAM were involved in writing—review and editing; HGA, MN, II, MAM, HA, and AAA performed supervision. All authors have read and agreed to the published version of the manuscript. All authors read and approved the final manuscript.

Funding
This project was funded by Princess Nourah bint Abdulrahman University Research Supporting Project Number PNURSP2022R241, Princess Nourah bint Abdulrahman University, Riyadh, Saudi Arabia.

Availability of data and materials
The data that support the findings of this study are available on request from the corresponding author.

Declarations

Ethics approval and consent to participate
This article does not contain any studies with human participants or animals performed by any of the authors.

Informed consent
Not applicable.

Competing interests
The authors have no conflicts of interest to declare. They have provided disclosure of potential conflicts of interest.

Author details
[1]Laboratory of Georesources, Geoenvironment and Civil Engineering (L3G), Faculty of Sciences and Techniques, Cadi Ayyad University, Marrakesh, Morocco. [2]Geography Department, Faculty of Arts and Humanities, Tartous University, Tartous, Syria. [3]Geography Department, Faculty of Arts and Humanities, Damascus University, Damascus, Syria. [4]Geography Department, Faculty of Arts and Humanities, Tishreen University, Lattakia, Syria. [5]Data Science for Sustainable Earth Laboratory (Data4Earth), Sultan Moulay Sliman univercity, Beni Mellal, Beni Mellal-Khenifra, Morocco. [6]Department of Geography, College of Arabic Language and Social Studies, Qassim University, Buraydah 51452, Saudi Arabia. [7]Department of Geography, College of Arts, Princess Nourah Bint Abdulrahman University, Riyadh 11671, Saudi Arabia.

Received: 5 July 2022 Accepted: 2 October 2022
Published online: 15 October 2022

References

Abdı A, Bouamrane A, Karech T, Dahri N, Kaouachi A (2021) Landslide susceptibility mapping using GIS-based fuzzy logic and the analytical

hierarchical processes approach: a case study in constantine (North-East Algeria). Geotech Geol Eng 39(8):5675–5691
Abdo HG (2020) Evolving a total-evaluation map of flash flood hazard for hydro-prioritization based on geohydromorphometric parameters and GIS–RS manner in Al-Hussain river basin, Tartous Syria. Natural Hazards 104(1):681–703
Abdo HG (2022) Assessment of landslide susceptibility zonation using frequency ratio and statistical index: a case study of Al-Fawar basin, Tartous, Syria. Int J Environ Sci Technol 19(4):2599–2618
Abedini M, Ghasemian B, Shirzadi A, Bui DT (2019a) A comparative study of support vector machine and logistic model tree classifiers for shallow landslide susceptibility modeling. Environ Earth Sci 78(18):1–15
Abedini M, Ghasemian B, Shirzadi A, Shahabi H, Chapi K, Pham BT, Tien Bui D (2019b) A novel hybrid approach of bayesian logistic regression and its ensembles for landslide susceptibility assessment. Geocarto Int 34(13):1427–1457
Aditian A, Kubota T, Shinohara Y (2018a) Comparison of GIS-based landslide susceptibility models using frequency ratio, logistic regression, and artificial neural network in a tertiary region of ambon, Indonesia. Geomorphology 318:101–111
Ayalew L, Yamagishi H (2005) The application of GIS-based logistic regression for landslide susceptibility mapping in the Kakuda-Yahiko Mountains Central Japan. Geomorphology 65(1–2):15–31
Ballabio C, Sterlacchini S (2012) Support vector machines for landslide susceptibility mapping: the Staffora River Basin case study Italy. Math Geosci 44(1):47–70
Batar AK, Watanabe T (2021) Landslide susceptibility mapping and assessment using geospatial platforms and weights of evidence (WoE) method in the Indian Himalayan region: recent developments, gaps, and future directions. ISPRS Int J Geo Inf 10(3):114
Benchelha S, Aoudjehane HC, Hakdaoui M, El Hamdouni R, Mansouri H, Benchelha T, Alaoui M (2019a) Landslide susceptibility mapping: a comparison between logistic regression and multivariate adaptive regression spline models in the municipality of Oudka, Northern of Morocco. Int J Geotech Geol Eng 13(5):381–393
Benchelha S, Chennaoui Aoudjehane H, Hakdaoui M, El Hamdouni R, Mansouri H, Benchelha T, Layelmam M, Alaoui M (2019b) Landslide Susceptibility Mapping in the Municipality of Oudka, Northern Morocco: a comparison between logistic regression and Artificial Neural networks models. ISPRS Int Arch Photogramm Remote Sens Spa Inf Sc XLII-4/W12:41–49
Bonham-Carter A, Wright DF (1988) Integration of geological datasets for gold exploration in Nova Scotia. Photogramm Eng Remote Sens 54(11):1585–1592
Boualla O, Mehdi K, Fadili A, Makan A, Zourarah B (2019) GIS-based landslide susceptibility mapping in the Safi region, West Morocco. Bull Eng Geol Env 78(3):2009–2026
Bourenane H, Guettouche MS, Bouhadad Y, Braham M (2016) Landslide hazard mapping in the Constantine city, Northeast Algeria using frequency ratio, weighting factor, logistic regression, weights of evidence, and analytical hierarchy process methods. Arab J Geosci 9(2):154
Bousta M, Ait Brahim L (2018) Weights of evidence method for landslide susceptibility mapping in Tangier, Morocco. In: MATEC web of conferences 149, 02042. https://doi.org/10.1051/matecconf/201814902042
Brahim LA, Bousta M, Jemmah IA, El Hamdouni I, ElMahsani A, Abdelouafi A, Lallout I (2018) Landslide susceptibility mapping using AHP method and GIS in the peninsula of Tangier (Rif-northern morocco). In Matec Web of Conferences (Vol. 149, p. 02084). EDP Sciences
Brenning A (2005) Spatial prediction models for landslide hazards: review, comparison and evaluation. Nat Hazard 5(6):853–862
Carrara A, Cardinali M, Guzzetti F, Reichenbach P (1995) GIS technology in mapping landslide hazard. In Geographical information systems in assessing natural hazards. Springer, Dordrecht, pp 135–175
Chen W, Chai H, Sun X, Wang Q, Ding X, Hong H (2016) A GIS-based comparative study of frequency ratio, statistical index and weights-of-evidence models in landslide susceptibility mapping. Arab J Geosci 9(3):204
Chen W, Xie X, Wang J, Pradhan B, Hong H, Bui DT, Ma J (2017) A comparative study of logistic model tree, random forest, and classification and regression tree models for spatial prediction of landslide susceptibility. CATENA 151:147–160
Chen W, Panahi M, Tsangaratos P, Shahabi H, Ilia I, Panahi S, Li S, Jaafari A, Ahmad BB (2019) Applying population-based evolutionary algorithms and a neurofuzzy system for modeling landslide susceptibility. CATENA 172:212–231
Chen W, Sun Z, Zhao X, Lei X, Shirzadi A, Shahabi H (2020) Performance evaluation and comparison of bivariate statistical-based artificial intelligence algorithms for spatial prediction of landslides. ISPRS Int J Geo Inf 9(12):696
Conoscenti C, Ciaccio M, Caraballo-Arias NA, Gomez-Gutierrez A, Rotigliano E, Agnesi V (2015) Assessment of susceptibility to earth-flow landslide using logistic regression and multivariate adaptive regression splines: a case of the Belice River basin (western Sicily, Italy). Geomorphology 242:49–64
Dehnavi A, Nasiri Aghdam I, Pradhan B, Morshed Varzandeh MH (2015) A new hybrid model using step-wise weight assessment ratio analysis (SWARA) technique and adaptive neurofuzzy inference system (ANFIS) for regional landslide hazard assessment in Iran. CATENA 135:122–148
Dou J, Yunus AP, Bui DT, Merghadi A, Sahana M, Zhu Z, Pham BT (2019) Assessment of advanced random forest and decision tree algorithms for modeling rainfall-induced landslide susceptibility in the Izu-Oshima Volcanic Island, Japan. Sci Total environ 662:332–346
El Khattabi J, Carlier E (2004) Tectonic and hydrodynamic control of landslides in the northern area of the Central Rif Morocco. Eng Geol 71(3–4):255–264
El Hamdouni I, Brahim LA, El Mahsani A, Abdelouafi A (2022) The prevention of landslides using the analytic hierarchy process (AHP) in a geographic information system (GIS) environment in the Province of Larache Morocco. Geomat Environ Eng 16(2):77–93
El Jazouli A, Barakat A, Khellouk R (2019) GIS-multicriteria evaluation using AHP for landslide susceptibility mapping in Oum Er Rbia high basin (Morocco). Geoenvironmental Disasters 6(1):1–12
El Jazouli A, Barakat A, Khellouk R (2022) Geotechnical studies for landslide susceptibility in the high basin of the Oum Er Rbia river (Morocco). Geol Ecol Landsc 6(1):40–47
Elmoulat M, Ait Brahim L (2018) Landslides susceptibility mapping using GIS and weights of evidence model in Tetouan-Ras-Mazari area (Northern Morocco). Geomat Nat Haz Risk 9(1):1306–1325
Elmoulat M, Brahim LA, Elmahsani A, Abdelouafi A, Mastere M (2021) Mass movements susceptibility mapping by using heuristic approach case study: province of Tétouan (North of Morocco). Geoenviron Disasters 8(1):1–19
Es-smairi A, El Moutchou B, Touhami AEO (2021) Landslide susceptibility assessment using analytic hierarchy process and weight of evidence methods in parts of the Rif chain (northernmost Morocco). Arab J Geosci 14(14):1–18
Es-Smairi A, El Moutchou B, El Ouazani Touhami A, Namous M, Mir RA (2022) Landslide susceptibility mapping using GIS-based bivariate models in the Rif chain (northernmost Morocco). Geocarto Int. https://doi.org/10.1080/10106049.2022.2097322
Ghasemian B, Shahabi H, Shirzadi A, Al-Ansari N, Jaafari A, Kress VR, Ahmad A (2022) A robust deep-learning model for landslide susceptibility mapping: a case study of Kurdistan Province Iran. Sensors 22(4):1573
Gourfi A, Daoudi L (2019) Effects of land use changes on soil erosion and sedimentation of dams in semi-arid regions: example of N'fis watershed in western high atlas, Morocco. J Earth Sci Clim Change 10(513):2
Guzzetti F (2005). Landslide hazard and risk assessment (Ph. D. Thesis). University of Bonn, Bonn (371 pp).
Harmouzi H, Nefeslioglu HA, Rouai M, Sezer EA, Dekayir A, Gokceoglu C (2019) Landslide susceptibility mapping of the Mediterranean coastal zone of Morocco between Oued Laou and El Jebha using artificial neural networks (ANN). Arab J Geosci 12(22):1–18
He Q, Shahabi H, Shirzadi A, Li S, Chen W, Wang N, Ahmad BB (2019) Landslide spatial modelling using novel bivariate statistical based Naïve Bayes, RBF Classifier, and RBF Network machine learning algorithms. Sci Total Environ 663:1–15
Hollard H, Choubert G, Bronner G, Marchand J, Sougy J (1985) Carte géologique du Maroc, scale 1: 1,000,000. Serv. Carte géol. Maroc, 260(2).
Hong H, Liu J, Zhu AX, Shahabi H, Pham BT, Chen W, Bui DT (2017) A novel hybrid integration model using support vector machines and random subspace for weather-triggered landslide susceptibility assessment in the Wuning area (China). Environ Earth Sci 76(19):1–19

Hong H, Liu J, Bui DT, Pradhan B, Acharya TD, Pham BT, Ahmad BB (2018) Landslide susceptibility mapping using J48 Decision Tree with AdaBoost, Bagging and Rotation Forest ensembles in the Guangchang area (China). Catena 163:399–413
Hosseinalizadeh M, Kariminejad N, Chen W, Pourghasemi HR, Alinejad M, Behbahani AM, Tiefenbacher JP (2019) Spatial modelling of gully headcuts using UAV data and four best-first decision classifier ensembles (BFTree, Bag-BFTree, RS-BFTree, and RF-BFTree). Geomorphology 329:184–193
Huang J, Ling S, Wu X, Deng R (2022) GIS-based comparative study of the bayesian network, decision table, radial basis function network and stochastic gradient descent for the spatial prediction of landslide susceptibility. Land 11(3):436
Igmoulan B, Namous M, Amrhar M, Bourouay O, Ouayah M, Jadoud M (2022) A comparative study of different machine learning methods coupled with GIS for landslide susceptibility assessment: a case study of N'fis basin, Marrakesh High Atlas (Morocco). Arab J Geosci 15(11):1–18
Jaafari A, Panahi M, Mafi-Gholami D, Rahmati O, Shahabi H, Shirzadi A, Pradhan B (2022a) Swarm intelligence optimization of the group method of data handling using the cuckoo search and whale optimization algorithms to model and predict landslides. Appl Soft Comput 116:108254
Jaafari A, Janizadeh S, Abdo HG, Mafi-Gholami D, Adeli B (2022b) Understanding land degradation induced by gully erosion from the perspective of different geoenvironmental factors. J Environ Manage 315:115181
Kanungo DP, Sarkar S, Sharma S (2011) Combining neural network with fuzzy, certainty factor and likelihood ratio concepts for spatial prediction of landslides. Nat Hazards 59:1491–1512
Karmaoui A, Zerouali S, Ayt Ougougdal H, Shah AA (2021) A new mountain flood vulnerability index (MFVI) for the assessment of flood vulnerability. Sustain Water Resour Manag 7(6):1–13
Kim EH, Ko JH, Oh SK, Seo K (2019) Design of meteorological pattern classification system based on FCM-based radial basis function neural networks using meteorological radar data. Soft Comput 23(6):1857–1872
Kong C, Tian Y, Ma X, Weng Z, Zhang Z, Xu K (2021) Landslide susceptibility assessment based on different machine learning methods in Zhaoping County of Eastern Guangxi. Remote Sensing 13(18):3573
Kontoes C, Loupasakis C, Papoutsis I, Alatza S, Poyiadji E, Ganas A, Spanou N (2021) Landslide susceptibility mapping of Central and Western Greece, combining NGI and WoE Methods, with remote sensing and ground truth data. Land 10(4):402
Lei X, Chen W, Pham BT (2020) Performance evaluation of gis-based artificial intelligence approaches for landslide susceptibility modeling and spatial patterns analysis. ISPRS Int J Geo Inf 9(7):443
Luo W, Liu CC (2018) Innovative landslide susceptibility mapping supported by geomorphon and geographical detector methods. Landslides 15(3):465–474
Machichi, M. A., Saadane, A., & Guth, P. L. (2020, May). On the viability of Neural Networks for landslide susceptibility mapping in the Rif, North of Morocco. In 2020 IEEE International conference of Moroccan Geomatics (Morgeo) (pp. 1–6). IEEE.
Magliulo P, Di Lisio A, Russo F (2009) Comparison of GIS-based methodologies for the landslide susceptibility assessment. GeoInformatica 13(3):253–265
Manchar N, Benabbas C, Hadji R, Bouaicha F, Grecu F (2018) Landslide susceptibility assessment in Constantine region (NE Algeria) by means of statistical models. Studia Geotechnica Et Mechanica 40(3):208–219
Mathieu P (2002) Caractérisation des sols et de leurs propriétés hydrodynamiques pour la modélisation hydrologique en milieu semi-aride, Bassin versant du Tensift – Maroc, Mémoire de fin d'étude ENSAM DAA « Physique des surfaces naturelles et génie hydrologique » (ENSAR) Avril 2002-Septembre 2002
Meliho M, Khattabi A, Mhammdi N (2020) Spatial assessment of soil erosion risk by integrating remote sensing and GIS techniques: a case of Tensift watershed in Morocco. Environ Earth Sci 79(10):1–19
Michard A, Saddiqi O, Chalouan A, Frizon de Lamotte D (2008) Continental evolution: the Geology of Morocco. Springer, Berlin. https://doi.org/10.1007/978-3-540-77076-3
Micheletti N, Foresti L, Robert S, Leuenberger M, Pedrazzini A, Jaboyedoff M, Kanevski M (2014) Machine learning feature selection methods for landslide susceptibility mapping. Math Geosci 46:33–57. https://doi.org/10.1007/s11004-013-9511-0
Mohammed S, Abdo HG, Szabo S, Pham QB, Holb IJ, Linh NTT, Rodrigo-Comino J (2020) Estimating human impacts on soil erosion considering different hillslope inclinations and land uses in the coastal region of Syria. Water 12(10):2786
Nasir MJ, Ahmad W, Iqbal J, Ahmad B, Abdo HG, Hamdi R, Bateni SM (2022) Effect of the urban land use dynamics on land surface temperature: a case study of Kohat City in Pakistan for the period 1998–2018. Earth Syst Environ 6(1):237–248
Nefeslioglu HA, Gokceoglu C, Sonmez H (2008) An assessment on the use of logistic regression and artificial neural networks with different sampling strategies for the preparation of landslide susceptibility maps. Eng Geol 97(3–4):171–191
Nsengiyumva JB, Luo G, Nahayo L, Huang X, Cai P (2018) Landslide susceptibility assessment using spatial multi-criteria evaluation model in Rwanda. Int J Environ Res Public Health 15(2):243
Oh HJ, Pradhan B (2011) Application of a neuro-fuzzy model to landslide-susceptibility mapping for shallow landslides in a tropical hilly area. Comput Geosci 37(9):1264–1276
Ozer BC, Mutlu BEGÜM, Nefeslioglu HA, Sezer EA, Rouai M, Dekayir A, Gokceoglu C (2020) On the use of hierarchical fuzzy inference systems (HFIS) in expert-based landslide susceptibility mapping: the central part of the Rif Mountains (Morocco). Bull Eng Geol Env 79(1):551–568
Park NW (2015) Using maximum entropy modeling for landslide susceptibility mapping with multiple geoenvironmental data sets. Environ Earth Sci 73(3):937–949
Park S, Kim J (2019) Landslide susceptibility mapping based on random forest and boosted regression tree models, and a comparison of their performance. Appl Sci 9(5):942
Park JY, Lee SR, Lee DH, Kim YT, Lee JS (2019) A regional-scale landslide early warning methodology applying statistical and physically based approaches in sequence. Eng Geol 260:105193
Pham BT, Tien Bui D, Pourghasemi HR, Indra P, Dholakia M (2017a) Landslide susceptibility assessment in the Uttarakhand area (India) using GIS: a comparison study of prediction capability of naïve bayes, multilayer perceptron neural networks, and functional trees methods. Theor Appl Climatol 128:255–273
Pham BT, Bui DT, Prakash I, Dholakia M (2017b) Hybrid integration of Multilayer Perceptron Neural Networks and machine learning ensembles for landslide susceptibility assessment at Himalayan area (India) using GIS. CATENA 149:52–63
Pham BT, Prakash I, Bui DT (2018) Spatial prediction of landslides using a hybrid machine learning approach based on random subspace and classification and regression trees. Geomorphology 303:256–270
Pourghasemi HR, Rahmati O (2018) Prediction of the landslide susceptibility: which algorithm, which precision? CATENA 162:177–192. https://doi.org/10.1016/j.catena.2017.11.022
Powell MJ (1992) The theory of radial basis function approximation in 1990. Adv Numer Anal 1992:105–210
Rahali H (2019) Improving the reliability of landslide susceptibility mapping through spatial uncertainty analysis: a case study of Al Hoceima Northern Morocco. Geocarto Int 34(1):43–77
Rahman G, Bacha AS, Moazzam MFU, Rahman AU, Mahmood S, Almohamad H, Abdo HG (2022) Assessment of landslide susceptibility, exposure, vulnerability and risk in Shahpur Valley, Eastern Hindu Kush. Front Earth Sci. https://doi.org/10.3389/feart.2022.953627
Roccati A, Paliaga G, Luino F, Faccini F, Turconi L (2021) GIS-based landslide susceptibility mapping for land use planning and risk assessment. Land 10(2):162
Rouai M, Jaaidi EB (2003) Scaling properties of landslides in the Rif mountains of Morocco. Eng Geol 68(3–4):353–359
Rumellhart D (1986) Learning internal representations by error propagation Parallel Distrib. Process 1:318–362
Saha S, Sarkar R, Roy J, Hembram TK, Acharya S, Thapa G, Drukpa D (2021) Measuring landslide vulnerability status of Chukha, Bhutan using deep learning algorithms. Sci Rep 11(1):1–23
Semlali I, Ouadif L, Bahi L (2019) Landslide susceptibility mapping using the analytical hierarchy process and GIS. Curr Sci 116(5):773–779

Shahabi H, Khezri S, Ahmad BB, Hashim M (2014) Landslide susceptibility mapping at central Zab basin, Iran: a comparison between analytical hierarchy process, frequency ratio and logistic regression models. CATENA 115:55–70
Shahabi H, Hashim M, Ahmad BB (2015) Remote sensing and GIS-based landslide susceptibility mapping using frequency ratio, logistic regression, and fuzzy logic methods at the central Zab basin Iran. Environ Earth Sci 73:8647. https://doi.org/10.1007/s12665-015-4028-0
Silalahi FES, Arifianti Y, Hidayat F (2019) Landslide susceptibility assessment using frequency ratio model in Bogor, West Java, Indonesia. Geosci Lett 6(1):1–17
Soma AS, Kubota T (2018) Landslide susceptibility map using certainty factor for hazard mitigation in mountainous areas of Ujung-loe watershed in South Sulawesi. For Soc 2:79–91
Song Ruhua HD, Kazutoki A (2008) Modeling the potential distribution of shallow-seated landslides using the weights of evidence method and a logistic regression model: a case study of the Sabae Area Japan. Int J Sediment Research 23(2):106–118
Tien Bui D, Tuan TA, Klempe H, Pradhan B, Revhaug I (2016) Spatial prediction models for shallow landslide hazards: a comparative assessment of the efficacy of support vector machines, artificial neural networks, kernel logistic regression, and logistic model tree. Landslides 13:361–378
Tien Bui D, Shahabi H, Shirzadi A, Chapi K, Alizadeh M, Chen W, Tian Y (2018) Landslide detection and susceptibility mapping by airsar data using support vector machine and index of entropy models in cameron highlands, malaysia. Remote Sens 10(10):1527
Tien Bui D, Shirzadi A, Shahabi H, Geertsema M, Omidvar E, Clague JJ, Lee S (2019) New ensemble models for shallow landslide susceptibility modeling in a semi-arid watershed. Forests 10(9):743
Tien Bui D, Pradhan B, Lofman O, Revhaug I (2012) Landslide susceptibility assessment in vietnam using support vector machines, decision tree, and Naive Bayes Models. Math Probl Eng. https://doi.org/10.1155/2012/974638
Tseng CM, Lin CW, Hsieh WD (2015) Landslide susceptibility analysis by means of event-based multi-temporal landslide inventories. Nat Hazards Earth System Sci Discuss 3(2):1137–73
Vapnik VNJT (1995) The Nature of Statistical Learning. Springer-Verlag, New York, NY
Varnes DJ (1978) Slope movement types and processes. Special Rep 176:11–33
Wang Z, Brenning A (2021) Active-learning approaches for landslide mapping using support vector machines. Remote Sens 13(13):2588
Wang LJ, Guo M, Sawada K, Lin J, Zhang J (2015) Landslide susceptibility mapping in Mizunami City, Japan: a comparison between logistic regression, bivariate statistical analysis and multivariate adaptive regression spline models. CATENA 135:271–282
Wang Y, Song C, Lin Q, Li J (2016a) Occurrence probability assessment of earthquaketriggered landslides with Newmark displacement values and logistic regression: the Wenchuan earthquake, China. Geomorphology 258:108–119
Wang LJ, Guo M, Sawada K, Lin J, Zhang J (2016b) A comparative study of landslide susceptibility maps using logistic regression, frequency ratio, decision tree, weights of evidence and artificial neural network. Geosci J 20(1):117–136
Wang G, Lei X, Chen W, Shahabi H, Shirzadi A (2020a) Hybrid computational intelligence methods for landslide susceptibility mapping. Symmetry 12(3):325
Wang X, Zhang Y, Atkinson PM, Yao H (2020b) Predicting soil organic carbon content in Spain by combining landsat TM and ALOS PALSAR images. Int J Appl Earth Obs Geoinf 92:102182
Yao X, Tham LG, Dai FC (2008) Landslide susceptibility mapping based on support vector machine: a case study on natural slopes of Hong Kong China. Geomorphology 101(4):572–582
Yilmaz I (2009) Landslide susceptibility mapping using frequency ratio, logistic regression, artificial neural networks and their comparison: a case study from Kat landslides (Tokat—Turkey). Comput Geosci 35(6):1125–1138
Yousefi S, Mirzaee S, Almohamad H, Al Dughairi AA, Gomez C, Siamian N, Abdo HG (2022) Image classification and land cover mapping using sentinel-2 imagery: optimization of SVM parameters. Land 11(7):993
Yu L, Cao Y, Zhou C, Wang Y, Huo Z (2019) Landslide susceptibility mapping combining information gain ratio and support vector machines: a case study from Wushan segment in the Three Gorges Reservoir area China. Appl Sci 9(22):4756
Zeybek M, Şanlıoğlu İ (2020) Investigation of landslide detection using radial basis functions: a case study of the Taşkent landslide Turkey. Environ Monitoring Assess 192(4):1–19
Zhang G, Cai Y, Zheng Z, Zhen J, Liu Y, Huang K (2016) Integration of the statistical index method and the analytic hierarchy process technique for the assessment of landslide susceptibility in Huizhou China. Catena 142:233–244
Zhang TY, Han L, Zhang H, Zhao YH, Li XA, Zhao L (2019) GIS-based landslide susceptibility mapping using hybrid integration approaches of fractal dimension with index of entropy and support vector machine. J Mt Sci 16(6):1275–1288
Zhang Y, Tang J, Cheng Y, Huang L, Guo F, Yin X, Li N (2022) Prediction of landslide displacement with dynamic features using intelligent approaches. Int J Min Sci Technol 32(3):539–549
Zhao S, Zhao Z (2021) A comparative study of landslide susceptibility mapping using SVM and PSO-SVM models based on Grid and Slope Units. Math Probl Eng. https://doi.org/10.1155/2021/8854606

Publisher's Note